Significance of Dielectric and Mechanical Properties on Fiber Loading of Sunn Hemp Reinforced Epoxy Composite

Chinmayee Dash[1, a)] and Dillip Kumar Bisoyi[1, b)]

[1] *Department of Physics and Astronomy, National Institute of Technology Rourkela, India-769008*

[a)]dash2016.chinmayee@gmail.com
[b)]Corresponding author: dkbisoyi@nitrkl.ac.in

Abstract. The mechanical and dielectric properties of Natural Sunn Hemp Fiber-reinforced Epoxy Composite with various fiber loadings are investigated at ambient temperature. Inadequate fiber loading decreases the mechanical strength of the composite. Dielectric constant and loss factor are increased with loading. The presence of non-debye type of relaxation was confirmed from the cole-cole impendence plot. Conduction mechanism in the composite system revealed the increase of conductivity values with an increase in fiber loading which ascribed to the addition of hydroxyl polar group in the amorphous phase. The study revealed that there is a correlation between structure and dielectric as well as mechanical properties exist.

INTRODUCTION

Use of Natural Fiber Reinforced Composites (NFRC) materials in the direction of inventing various engineering materials have become the greatest interest from the last couple of years. It provides lightness, high strength, toughness, good corrosion resistance to final end-use products and also a good insulation medium to some special appliances like switchboards, electrical cable, protecting coatings on electrical wires and cables, bushings, etc.[1]. Natural fibers (NF) also have proven as a replacement of synthetic fiber in the use of developing electrical as well as electronic goods. The discard various electronics devices like computer and TV monitors, printed circuit boards, plastics from printers, keyboards, electronics wires in many developing countries adversely affecting the biological ecosystem[2]. Release of toxic phosphorous from TVs and computers, brominated dioxins from plastics are very much harmful to the environment and their involvement in communities is risky since their non-biodegradability and non-recyclability nature. To use NF in the motive of fabricating various products, it is crucial to investigate their behavior towards various mechanical and dielectric parameters as they possess polar OH group and are semicrystalline in character. The dielectric as well as mechanical properties of NFRC varies fiber to fiber depending upon their chemical composition and are also affected by certain factors that exhibit by raw natural fibers (NF) themselves such as high absorbance of water, wide variety of fibers, fiber encumbering, different fiber aspect ratio, composite processing, fiber extraction etc[3]. The polar groups are responsible for polarization in the presence of the applied electric field while the fiber crystallinity provides strength and stiffness to the composites. Some fruitful investigations have been accomplished on various NFRC to explore their sensitivity towards different polarization as well as different dielectric parameters [4, 5, 6]. The literature review suggests there are very least reported articles that report about the dielectric response towards sunn hemp reinforced epoxy composite. Sunn hemp (Crotalaria Juncea) comes under the bast fiber family. This fiber contains a high amount of cellulose (70-78 wt %) after cotton fiber (82-90 wt %), density (1.4-1.6 g/cm^3), aspect ratio (450), due to which it holds superior mechanical property that is much beneficial for field carrying conductor[7]. So the current work will signify on the effect of frequency-dependent dielectric parameters and mechanical behavior on various fiber loading of sunn hemp fiber reinforced epoxy composite. The study of fiber loading on the composite is a leading point to sense the dielectric behavior since the polar hydroxyl (-OH) group present in carbohydrates and other noncellulose parts is controlled by the applied field. So increasing the fiber content

add more number of polar groups and hence the properties of composite vary accordingly. In addition to that, a parallel discussion has also been made on the effect of ac conductivity (σ_{ac}) and impedance study.

MATERIALS AND METHODOLOGY

The sunn hemp fiber was collected from Central Research Institute for Jute and Allied Fibers (CRIJAF), Kolkata, India. The epoxy resin (L12, density=1.17g/cm^3)and curing agent hardener (K6, density=0.98 g/cm^3) were collected from Himedia Laboratories Pvt. Ltd, Mumbai, India. The fiber was cleaned and vacuum dried at 80° temperature prior to preparing the composites, designated as 'Raw Sunn Hemp (RSH)' fiber. The composites for the dielectric and mechanical test were prepared by hand layout technique. Epoxy resin was pre-sonicated and degassed at 80° under vacuum. After a modest cooling of epoxy, hardener (Epoxy:Hardener=10:1 by weight) was mixed and stirred at least for 5-7 minutes. RSH fiber of 5, 10, 15, 20 and 25 volume percentage was chopped, mixed with epoxy/hardener solution and stirred for 5 to 7 minutes until to get a homogeneous blending. The mixture was then poured in heavy-duty silicon sprayed cylindrical plastic mold of 15 mm diameter for dielectric measurement. The composites for the 3 point bending test of dimension (100×12×5) mm^3 and tensile test of dimension (165×19×5) mm^3 were prepared according to the ASTM-D3039 and ASTM-D7264 standard respectively in a rectangular mold. Air bubbles were avoided by pressing the molded mixture with the help of a glass tube in the earlier process where an iron roller was used for the latter and cured at room temperature for 24 hours. The obtained composites were designated as RSHC5, RSHC10, RSHC15, RSHC20 and RSHC 25 where the number denotes the number of fiber loadings. X-ray Diffraction (XRD) pattern of sunn hemp fiber was recorded by CuKα radiation Ultima IV- Rigaku, Japan diffractometer. Data were taken at 2θ range of 5˚- 50˚ and scanning rate of 3˚/min with step size 0.01. The microstructure images of fractured composites' surface were carried out by using FESEM (Nova Nanosem 450, Japan) at 10KV accelerating voltage. The mechanical test was performed by a Universal Testing Machine (Instron-5967, UK) with Environmental Chamber at a loading rate of 3mm/min. The top and bottom surface of dielectric specimens were coated with conductive silver paste and the measurement was prosecuted at ambient temperature using a HIOKI LCR meter (Im-3533-01) with varying frequency from 100 Hz to 100 kHz. The dielectric parameters from the measurement can be calculated from the following formulations.

$$\varepsilon' = \frac{C}{C_o} \text{ where } C_0 = \frac{\varepsilon_0 A}{d}, \tan\delta = \frac{\varepsilon''}{\varepsilon'}, \quad \sigma_{ac} = \omega\varepsilon\varepsilon_0\tan\delta, \quad Z' = Z\cos\varphi \text{ and } Z'' = Z\sin\varphi \tag{1}$$

where ε is complex dielectric constant, ε' *and* ε'' are real and imaginary dielectric constant, ε_o is the dielectric permittivity of air (8.85×10^{-12} F/m), ω is the angular frequency, σ_{ac} is ac conductivity, Z is the complex impedance, $Z'$and Z'' are real and imaginary impedance and φ is the phase.

RESULTS AND DISCUSSIONS

Figure1 (a) shows the plot of the XRD pattern of RSH fiber where two pronounced peaks at Bragg's angle of 15.6˚, 22.6˚ and one depressed peak at the angle of 34.7˚ are observed which attributed to [101], [002] and [040] respectively.

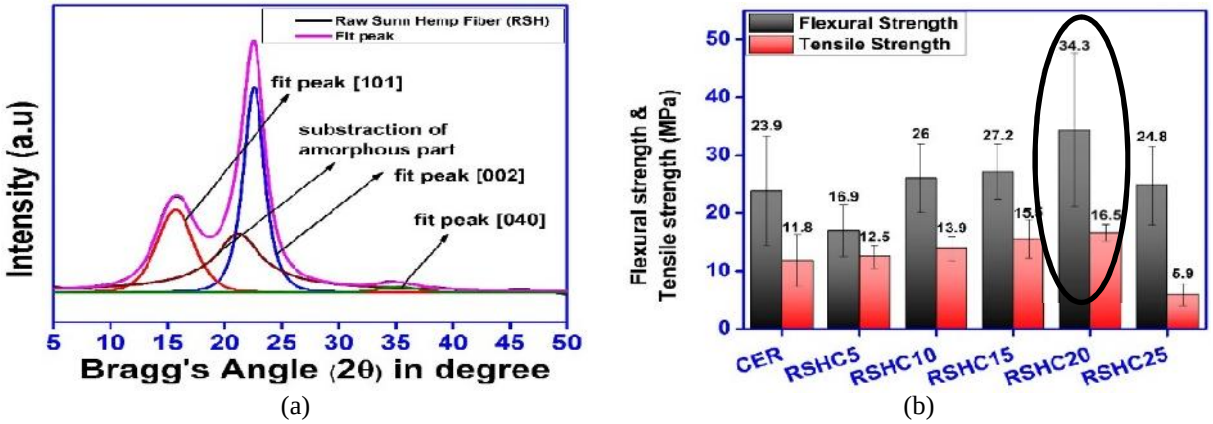

FIGURE 1. (a) XRD pattern of RSH b) Mechanical strength of RSHC of various fiber loadings

These peaks are related to crystalline cellulose I and the minimum intensity region near 2θ=18˚ is from noncellulosic amorphous compositions. As a naturally occurring fiber, Sunn Hemp possesses a higher amount of cellulose in comparison to other noncellulosic components so is a bi-phase material. In fiber, the arrangement of the polymer chain in such a way that some region exhibits a high degree of chain order forms a crystalline phase wherein some region there is some short length chain pass among these ordered chain regions which form amorphous phase. Since the cellulose is an amalgamation of both ordered and disordered chains, so the diffracted pattern comes with a smeared one. So taking the smearing and skewness of peak shape into consideration, each peak profile is fitted using Pearson VII function which is in the form of

$$I = \frac{A}{1+\left(\frac{x-X_c}{w}\right)^2 (2^{\frac{1}{\mu}}-1)} \quad (2)$$

Where I is Intensity, x is Bragg's angle, Xc is Bragg's angle of peaks and μ is profile shape factor, A is peak amplitude, w is full-width half maxima. The shape parameter μ determines the shape of particular peak tails that is μ=1 (Cauchy shape), μ=2 (Modified Lorentzian shape), μ=.∞ (Gaussian shape)[8]. The fitting parameters for 101, 002 and 040 reflection planes were extracted individually and shown in table 1. From the table, we observed the peak shape is a composite of Gaussian and modified Lorentzian types. The obtained amplitudes A is the composition of these two peaks. The cellulose crystallinity and apparent crystallite size are calculated using Segals's peak height method and Schere's formula which are found to be 72% and 31.2 Å. Hence, RSH fiber possesses enough crystalline domain which makes the fiber mechanically strong.

TABLE 1. Pearson VII function fitted parameters of three peaks for RSH fiber

Samples	Planes of reflections	2θ=X_c	A	w	m
RSH	101	15.6	53109.7	3.8	3.5
	002	22.6	86340.6	2.2	1.9
	040	34.7	3385.4	3.9	170

Figure. 1 (b) shows the mechanical strength of various fiber-loaded composites. Result obtained that incorporation of 20% fiber into the matrix is providing best flexural strength (34.3 Mpa) and tensile strength (16.5 MPa). As fiber packing was further increased from 20% to 25%, the developed composite saw a gradual fall of flexural strength from 34.8 Mpa to 24.8 Mpa and tensile strength from 16.5 Mpa to 5.9 MPa. The higher value of mechanical strength acquired by RSHC20 where the result can be clarified on the justification of adequate mixing of fiber with matrix, parallel stress transfer from matrix to fiber, appropriate wetting of fiber leading less void formation in matrix region and better crosslinking between the matrix and cellulose chains of fiber. As fiber packing increases, the failure of mechanical performance in the composite arise which put down to improper gathering of fiber and matrix by the inclusion of the disproportionation of fiber that blocks the path for penetration of resin into fiber and causes inappropriate fiber wetting. High insertion of fiber might hinder crosslinking from interlocking with the chain of the polymer matrix which causes a weak interface.

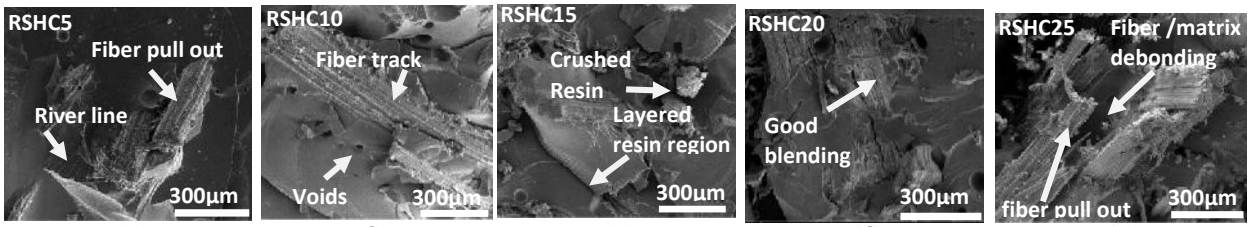

(a) (b) (c) (d) (e)

FIGURE 2. Microstructure images of fractured surface of surfaces for (a) RSHC5 (b) RSHC10 (c) RSHC15 (d) RSHC20 (e) RSHC25

In Figure. 2, RSHC5 show very minimal amount of fiber dispersion within high concentration resin region which form matrix dominating river lines that provide the information about crack growth propagation in the composite[9].

There is also some fiber pull out observed from resin due to poor fiber /matrix adhesion. In fig. 2(b), the RSHC10 shows a complete pull out of fiber from its track with mark left behind by imprinting which indicates poor stress transformation from matrix to reinforcement lead to poor fiber/matrix adhesion. Poor bonding leads to voids and porosity that is clearly observed in the resin surface which might be due to moisture presence and air molecule trapped during the processing of the composite or heavy crosslinking between thermosetting epoxy with fibers during cure. Porosity and voids are the weakness that causes a reduction in the mechanical performance of the composite. In fig. 2(c), the RSHC15 shows the splitting of matrix surface into layers due to the more number of pulled out fiber from the interior resin region. In some places, epoxy resin has crashed due to heavy pull out of fibers which form resin aggregates on the fracture surface and it directly leads to the formation of the thermosetting rich region.RSHC25 has the most number of fiber pullout along with fiber/matrix debonding. Large inclusion of fiber act as stress concentration promoting failure and lower the toughness. Comparative to other fractography, RSHC20 show very less amount of fiber pull out. Adequate wetting of sunn hemp fibers and a good blending within the epoxy were observed which admitted with our previously obtained mechanical results.

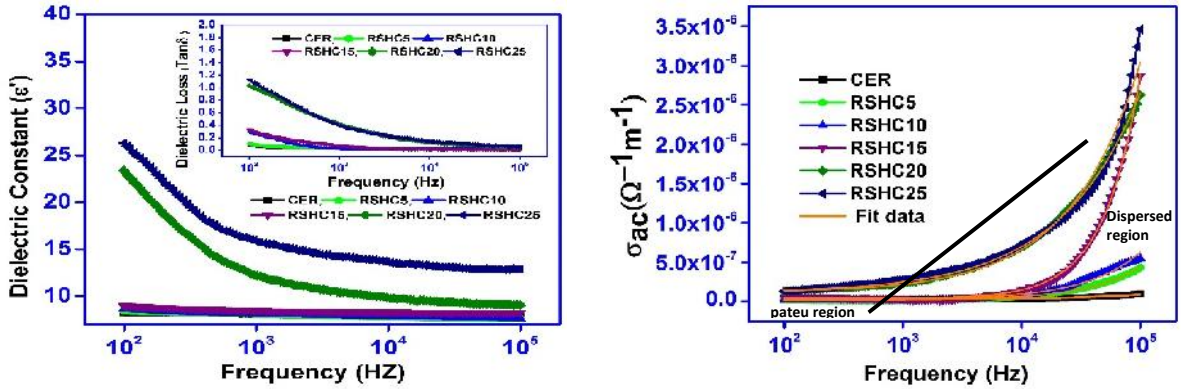

FIGURE 3. Frequency dependence (a) dielectric constant (Inset: loss factor) (b) ac conductivity (Inset: frequency component plot) of RSHC with various fiber loadings.

Figure. 3 (a) depicts frequency dependence ε' and $Tan\ \delta$ (inset) of the fiber-loaded composites. Both figures show an increasing trend over the entire frequency range and the ε' and $Tan\ \delta$ values increase with the increase in fiber loading. This simultaneous increment and dispersion of spectrum at lower range frequencies suggests the addition of more polar groups that are available in fiber constituents and also is a consequence of Maxwell-Wagner-Sillars (MWS) interfacial polarization. The amorphous phase in the fiber polymer chain takes charge of the current flow through the entire composite. So rising the fiber population in resin ultimately add the number of polar groups in composite and expand the amorphous phase which tends to increase the ε' and $Tan\ \delta$ values. It is noticed that RSHC5, RSHC10 and RSHC15 exhibit a very minimal variation in ε' and $Tan\ \delta$ values from each other which might be due to a low fractional amount of fiber in the composite that leaves voids at fiber/matrix interface. Cured epoxy resin (CER) exhibit almost very less ε' and $Tan\ \delta$ values and very much comparable to those of RSHC5, RSHC10 and RSHC15 which is attributed to the nonpolarity and hydrophobic characteristic of the polymer chain that controls the instantaneous atomic and electronic polarization. The sudden and significant catastrophic augmentation of ε' and $Tan\ \delta$ values from RSHC15 to RSHC20 and RSHC25 may indicate the availability of submerged polar (-OH) groups in the fiber constituents. Incorporation of high volume fractional fiber into matrix may able to overcome the voids in the resin flow region and lead to an effective degree of interfacial and dipolar polarizability in the sample, which is more active at lower frequency region rather than higher frequency due to incomplete rotation of dipoles and conformational motion of polymer amorphous chains. The gradual increment of $Tan\ \delta$ values with the increase of fiber loadings suggests the accumulation and consumption of current in the amorphous phase of semicrystalline fiber which dissipates in the form of heat energy therefore give rise to high loss which comes in a consistent way with conduction relaxation in ac conductivity (σ_{ac}) mechanism as shown in fig. 3(b).

In figure 3(b), the low-frequency dc plateau region and high-frequency ac dispersive region in the scene are due to the bulk conductivity of the composite and hoping process of mobile polar ions[10]. The simultaneous increment of σ_{ac} values with fiber loading follows an explanation of the pasting of more hydroxyl polar groups which acts as an electrical transport charge carrier. The low volume fraction of fiber dispersion within the matrix resin has less number of polar groups so possess a low value of conductivity. The short-ranged amorphous polymer chain is responsible for

charge transportation throughout the fiber so increasing the fiber population ultimately increases the number of polar groups in fiber. These polar groups lead to the absorbance of moisture within the fiber and increase the conductivity. To understand the viable electrical conduction mechanism in RSHC, the σ_{ac} spectrum is fitted using Jonscher's universal power-law $\sigma_{ac} = \sigma_{dc} + A\omega^s$, where σ_{dc} is dc conductivity, A and ω are dispersion parameter and angular frequency, s ($0<s<1$) is frequency component. We may notate that ions can tunnel from trapped crystalline region to the amorphous region through the interface and take part in the conduction process. Such a process may happen in the composite due to polymer chains translational motion at ambient temperature.

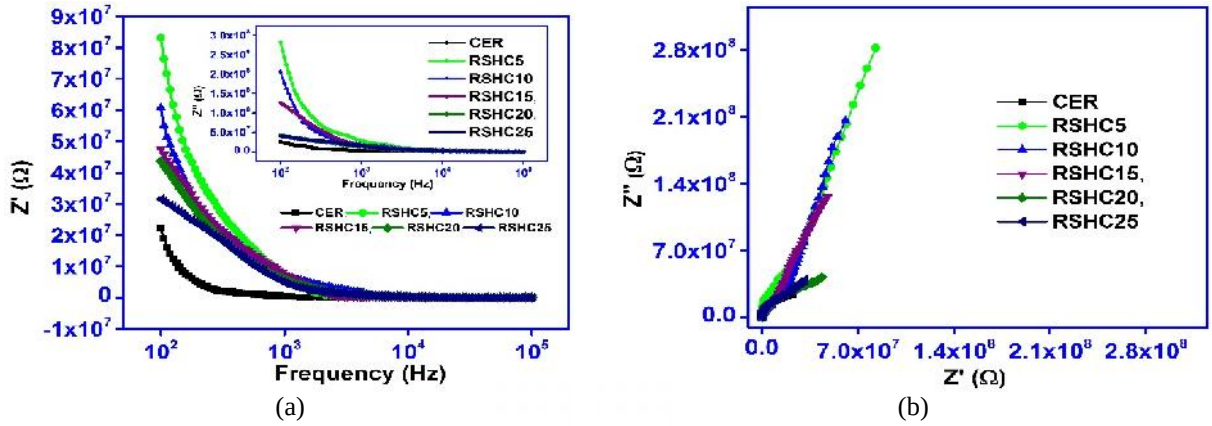

FIGURE 4. Frequency dependence (a) Z' (Inset: Z'') (b) Nyquist plot of RSHC with various fiber loadings.

Figure 4 (a) show frequency dependent Z' and Z'' plot with reference to fiber loading where they show an equivalent trend of increment with rising of fiber content and merged to a single line towards the higher frequency which indicates the free of space charge due to ineffectiveness of mobile charge orientation. The decrease in Z' and Z'' magnitudes with the growth of fiber insertion follow the explanation of the promotion of conduction in RSHC by applied alternating current field which is due to the availability of more polar groups in fiber due to high insertion of fiber into resin and entry of foreign as well as local impurities. The high fiber population into resin also form agglomeration at the interface that reduces the internal resistance between the fibers and lead to the lowering of Z' and Z'' values. The non-polarity in CER gives rise to the lowest Z' and Z'' values. From fig. 4 (b), the cole-cole plot displays the trend from linear to semicircles and lowering of these semicircles with their diameter which signifies the existence of non-debye type of relaxation.

CONCLUSIONS

The mechanical and dielectric behavior of Sunn Hemp Reinforced Epoxy Composite as a reference of various fiber loading (5, 10, 15, 20 and 25vol%) were studied. From the X-Ray diffractogram, it was found that Sunn Hemp fiber possesses a high degree of crystallinity which is a key factor to control the mechanical strength of the composite. The mechanical result of the composite specimen showed that the incorporation of 20vol% of fiber (RSHC20) yield a better flexural as well as tensile strength. ε' and $Tan\ \delta$ values are observed to be increased with the increase of fiber loadings. The ac conductivity analysis of composite resulted in an increasing magnitude along with the fiber loading and revealed the growth of charge transport carriers in the amorphous phase upon the addition of fiber. The Nyquist plot shows the deviation from debye relaxation in all the composites. The mechanical and dielectric properties of RSHC specimens are correlated structurally.

ACKNOWLEDGMENT

The authors express their sincere gratitude to the Director, National Institute of Technology Rourkela, Rourkela-769008, India for bestowing the fellowship and allowing to carry out this research work with availability infrastructure facilities in the institute. Dr. Surendra Kumar Pandey, Principal Scientist, CSIR-Central Research Institute for Jute and Allied fibers (CSIR-CRIJAF), Barrackpore, Kolkata-700120, India is highly acknowledged for providing Sunn

Hemp fiber for research work. The authors also very much thankful to Dr. Sadhna Agrawal, Dept. of Physics, National Institute of Technology Raipur, Raipur-492013, India for her assistance in the dielectric measurement facilities.

REFERENCES

1. A. Patra and D. K. Bisoyi, J. Mater. Science 45, 5742–5748 (2010).
2. H. B. Bhuvaneswari, D. L. Vinayaka, M. Ilangovan, and N. Reddy, J. Mater. Science: Mater. Electron 28, 12383–12390 (2017).
3. K. L. Pickering, M. G. A. Efendy, and T. M. Le, Composites : Part A 83, 98–112 (2016).
4. A. Triki, M. Guicha, M. Ben Hassen, M. Arous, and Z. Fakhfakh, J. Mater. Science 46, 3698–3707 (2011).
5. I. Ben Amor, H. Rekik, H. Kaddami, M. Raihane, M. Arous, and A. Kallel, J. Electrostatics. 67,717–722, (2009).
6. P. Li, Y. Tao, and S. Q. Shi, BioResources 9, 2681–2688 (2014).
7. M. Liu, A. Thygesen, J. Summerscales, and A. S. Meyer, Ind. Crops Products 108, 660–683 (2017).
8. S. K. Gupta, J. Appl. Crystallography 31, 474–476 (1998).
9. Emile S. Greenhalgh, *CRC Press* (Woodhead Publishing Limited, New York, 2009), pp. 356-440
10. I. Ben Amor, Z. Ghallabi, H. Kaddami, M. Raihane, M. Arous, and A. Kallel, J. Mol. Liquids 154, 61–68 (2010).